Heliyon 8 (2022) e11695

Contents lists available at ScienceDirect

Heliyon

journal homepage: www.cell.com/heliyon

Research article

Additive manufactured polymeric shock absorbers for automotive applications

A. Riccio *, M. Madonna, C. Palumbo, A. Sellitto

Department of Engineering, Università degli Studi della Campania "Luigi Vanvitelli", via Roma n 29, Aversa (CE), Italy

ARTICLE INFO

Keywords:
Shock absorbers
Additive manufacturing
FEM
Automotive
Nonlinear model

ABSTRACT

This paper deals with the use of shock absorbers, placed in the upper roof of vehicles, able to increase the safety of passengers during an impact event. Numerical impact analyses have been introduced to demonstrate the effectiveness of these shock absorbers by assessing the deformations, stress and energy dissipation capabilities in the different structural components of a vehicle, somehow related to the safety of passengers. Indeed, shock absorbers have been found to play an important role in relation to passengers' safety. The homologation limitations of the reference regulation have been taken into account: FMVSS No. 201U "internal head impact – passenger compartment". This regulation, actually, provides a fundamental parameter, known as HIC(d) – "Head Injury Criteria", which is strictly related to the injuries of the passenger head under impact conditions alongside the rigid components inside the vehicle. The HIC(d) threshold value, if exceeded, affects the final conformity test of a vehicle. Hence, to fall within the range of reliable values of the HIC(d), shock absorbers need to be adopted. In order to increase these shock absorbers efficiency, in terms of passenger safety, in compliance with the regulations, the possibility of production of such devices by additive manufacturing techniques has been assessed.

1. Introduction

This work is focused on impact analysis, specifically "internal head impact" analysis for automotive applications. This study considerers shock absorbers according to National Highway Traffic Safety Administration (NHTSA) organization standards [1]. According to crashworthiness requirements, an essential step for vehicles' certification is the assurance of increased safety for passengers involved hard impacts by introducing specific active and passive safety devices [2]. Active safety systems are activated just before the impact event to avoid catastrophic consequences. These systems include automatic emergency braking, rear cross-traffic alert, forward collision warning. Other active safety devices are the brakes, the lights, the steering wheel, the electronic devices such as ABS (Anti Brake-Locking System) which operates the braking system to prevent locking of the wheels, and ESP (Electronic Stability Control) [3].

Passive safety systems are aimed to reduce the damage caused by impacts; examples of passive safety systems are airbags, seat belts and head restraints. According to these passive safety principles, all the vehicle components are designed to absorb the impact deformation energy to avoid relevant damages to the passenger compartment. The National Highway Traffic Safety Administration (NHTSA) is the division of the United States Department of Transportation which has the role of investigating safety defects in motor vehicles, setting and enforcing fuel economy standards, helping states and local communities to reduce accidents, promoting the use of safety belts, child safety seats and air bags, conducting researches on driver behaviour and traffic safety, and providing consumer information on motor vehicle safety topics [4, 5]. The test procedures are delivered by NHTSA Office of Vehicle Safety Compliance (OVSC), with the main purposes of presenting guidelines for uniform testing standards and data recording formats and providing suggestions for the use of specific equipment and procedures for testing laboratories [6]. In this work, a specific requirement has been considered: Federal Motor Vehicle Safety Standard (FMVSS) No.201 concerning the Occupant Protection in Interior impact. This requirement [7, 8] applies to passenger cars, trucks, buses, and multipurpose passenger vehicles (MPVs) with a gross vehicle weight rating (GVWR) of 4536 kg or less. Two possible compliance options can be selected: FMH Impact Speed or Reduced FMH Impact Speed [7]. In particular, according to the FMH Impact Speed compliance option, each tested vehicle must comply with the requirements underlying at all target locations when impacted by the Free Motion Headform (FMH) at any speed up to and including 24 km/h (15 mph) [9]. To fulfil these requirements, shock absorber structures are

* Corresponding author.
E-mail address: Aniello.Riccio@unicampania.it (A. Riccio).

https://doi.org/10.1016/j.heliyon.2022.e11695
Received 13 May 2022; Received in revised form 13 July 2022; Accepted 10 November 2022

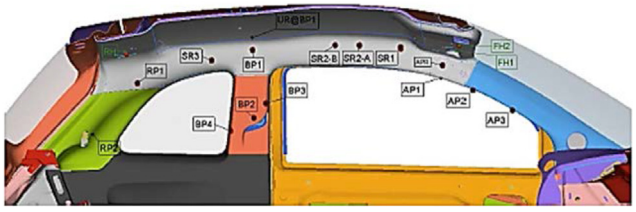

Figure 1. Upper Roof Graphical Explanation with target location.

usually adopted at all the target locations. In [10], an analytical model is presented for the calculation of mean crush force in Free Motion Headform Impactor for transport applications. In order to reduce impact force peaks, the high capability of metallic materials to dissipate the absorbed energy by plastic deformation has been used in [11], by introducing the state of the art of metallic shock absorber systems [11, 12] or thin walled metallic mechanisms [13]. These metallic shock absorbers, even if very effective in reducing the impact peak forces, have been found to significantly increase the vehicle weight. Moreover, their energy absorption capabilities are influenced by different design parameters, as their shape and thickness [14]. However, variations of the shape and thickness are restricted by the traditional manufacturing techniques, limiting the possibilities in terms of design and material distribution in the components designed to be optimized to the energy absorption tasks. Hence, in order to develop solutions able to provide superior energy absorption characteristics, innovative manufacturing techniques, as the additive manufacturing (AM), must be taken into account. According to this technology, complex geometries can be 3D printed in both metallic and polymer materials [15, 16], leading to the development of new and more efficient energy absorbing systems. The innovative concept of designing shock absorber oriented to the AM is the focal point for this paper, where a new paradigm for variable density material distribution has been attempt by adopting additive manufacturing unique features without the use of specific fixed moulding devices.

In the frame of this work, authors numerically investigated, in a preliminary design stage, on the use of polymeric shock absorbers designed for additive manufacturing specifically aimed to increase specific energy absorption characteristics and to reduce force peaks in the main critical vehicle components, as a consequence to interior head impact, compared to traditionally manufactured shock absorber. Exploiting the possibility of AM, an optimization procedure has been performed to determine the optimal shock absorber configuration able to maximize its energy absorption capability. Moreover, the use of AM polymers results in components lighter than the traditional metallic ones, which has positive effects in terms of weight and consequently emission reduction, in accordance to the environmental safeguard legislation constraints. Follow-on experimental activities will be focused on the testing of the prototype produced by using AM technology, according to the optimal design configuration.

In Section 2, the test procedure and the requirements for Head Interior Impacts, to be fulfilled in terms of safety, are presented. In Section 3, a description of the numerical procedure, adopted in the frame of this research work for the assessment of the new polymeric shock absorber, is provided. Finally, in Section 4, the results from the virtual simulations with and without additive manufactured polymeric shock absorbers, together with the results from an optimization analysis on the shock absorbers design, are presented and discussed.

2. Test procedure and requirements for head interior impacts

The manufacturer's data supplied by the Contracting Officer's Representative (COR) is used to locate the Seating Reference Points (SgRP) by determining their coordinates, after which the coordinates for head C.G. of the forward front seat position (CG-F1), the aft front seat position (CG-F2) and rear seat position (CG-R) on both driver and passenger sides of the test vehicle are determined by specific locations. In Figure 1, a graphically explanation with upper interior components and their relative target locations is shown.

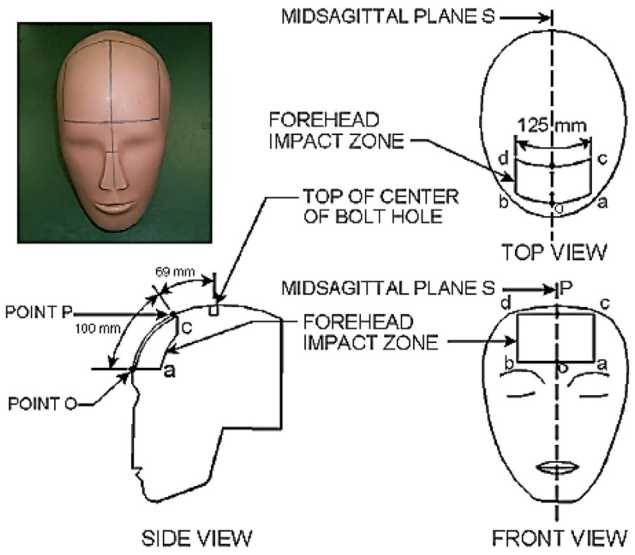

Figure 2. FMH forehead impact zones.

Each of these points (the same as for FMH approach angles) are determined through specific procedures, involving intersections of lines obtained by many planes orthogonal intersections with the vehicle. Figure 2 illustrates the forehead impact zone.

The FMH forehead impact zone and angles are determined in accordance with the following procedure [17]:

- The headform is positioned so that the baseplate of the skull is horizontal. The midsagittal plane of the headform is designated as Plane S.
- From the centre of the threaded hole on top of the headform, a 69 mm line forward toward the forehead is drawn, coincident with Plane S, along the contour of the outer skin of the headform.
- The front end of the line is designated as Point P. From Point P, a 100 mm line forward toward the forehead is drawn, coincident with Plane S, along the contour of the outer skin of the headform. The front end of the line is designated as Point O.
- A 125 mm line is drawn, coincident with a horizontal plane along the contour of the outer skin of the forehead from left to right through Point O so that the line is bisected at Point O. The end of the line on the left side of the headform is designated as Point a, and the end of the right as Point b.
- Another 125 mm line is drawn, coincident with a vertical plane, along the contour of the outer skin of the forehead through Point P so that the line is bisected at Point P. The end of the line on the left side of the headform is designated as Point c and the end on the right as Point d.
- A line from Point a to Point c along the contour of the outer skin is drawn by using a flexible steel tape. The forehead impact zone is the surface area on the FMH forehead bounded by lines a-O-b and c-P-d, and a-c and b-d.

In order to calculate the limits to be observed by the competent authority, the HIC is calculated. The "Head Injury Criteria" HIC is estimated according to Eq. (1):

$$HIC = \left[\frac{1}{t_2 - t_1}\int_{t_1}^{t_2} A_r dt\right]^{2.5}(t_2 - t_1) \quad (1)$$

where $A_r = [A_x{}^2 + A_y{}^2 + A_z{}^2]^{1/2}$ is the resultant acceleration magnitude in g units at the dummy head CG, and t_1 and t_2 are any two points in time during the impact event which are separated by no more than a 36-

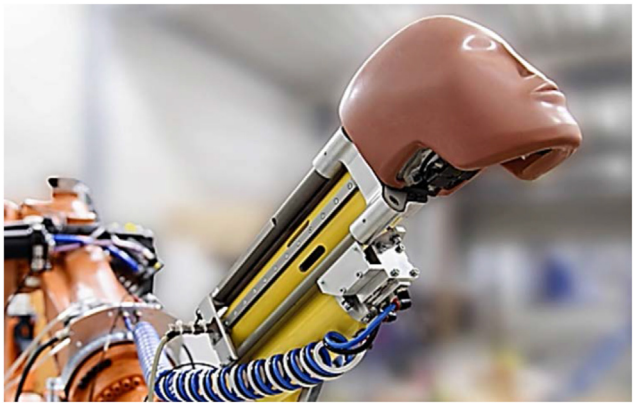

Figure 3. FMH installation.

millisecond time interval. HIC(d) shall not exceed 1000 when calculated in accordance with Eq. (2):

$$HIC(d) = 0.75446\ (\textit{Free Motion Headform HIC}) + 166.4 \quad (2)$$

Different measurements are obtained considering the headform attached or not attached (free motion) to a body. In particular, HIC(d) represents the HIC of a free motion headform; therefore, it is possible to conduct a test without needing to use the entire dummy. As stated above, dummies are used to evaluate the injuries on occupants during a crash event and as impactors for pedestrian safety. The Free Motion Headform (FMH) is a Hybrid III type dummy head used to assess occupant safety due to an impact in the interior of a vehicle. The FMH is launched from inside the vehicle so that its forehead strikes the selected target component (e.g., pillar, side rail, or header); integrated accelerometers are used to monitor the head response during the impact. These measurements are used to calculate the HIC injury criteria and the model is validated with Head Drop tests on to rigid and deformable sections against physical test data. The unit, as shown in Figure 3, has a vertical line laser mounted on top and projecting upward, while the forehead is scribed with a target pattern following the requirements of FMVSS 201 [18]. A digital protractor is mounted to the underside of the aluminium beam and a bubble level is used for cross axis angle zeroing.

The impactor is capable of pushing the FMH at the specified impact speed of 23.7 km/h ± 0.3 km/h, or 18.7 km/h ± 0.3 km/h, while providing the midsagittal plane of the FMH vertical and upright throughout launch to the instant of free flight. FMH impactor is equipped with a compact launcher capable of propelling it at any specified target and approach angle located within the test vehicle's occupant space. Its propulsion system is capable of producing highly accurate and repeatable FMH impacts. Compliance Test Execution is edited with the vehicle specifications; to measure its attitude, the vehicle is positioned on a flat and level horizontal surface, while, to facilitate targeting and placement of the FMH impactor, seats, windows and other components are removed.

The FMVSS No.201U approach consists of the following steps:

- Targeting and Testing: target points and impact conditions, according to regulations, are defined. The testing requirements of a valid impact condition are the impact zone, the target reachability achievability, the free head rotations (5/10 deg), the free flight conditions, etc.
- Selection: the design team, supported by the experience, provides the right, among the infinite, combination between the head approach angle and internal components.
- Worst cases identification: A screening of the available solutions is carried out; those cases considered most critical are identified, for example: minimum CRD, critical distance from rigid parts (body, return ring pins), minimum Head Deviation, the distance from the point O of the impact zone, minimum\maximum vertical angle according to the conditions or the type of target.
- Virtual simulation: numerical simulations of the head impact against internal components are performed, and the results in terms of head deceleration are monitored. These result values are read in a node placed in the head centre of gravity, and plotted on diagrams as a function of the time (a, t), to evaluate HIC(d) and acceleration peak. HIC(d) must not exceed the homologate limit of 1000. Critical issues, due to multiple possible head impact conditions against the passenger compartment, are evaluated.
- Experimentation: In the experimental phase, the predicted FEM values are assessed by comparison with experimental test results for each target location.
- Final report: Compliance test is ready to be drawn up.

In the frame of this work, only the virtual simulation has been taken into account for the sake of brevity. Hence, the most critical scenario has been investigated to test the performance of the shock absorbers, and the subsequent optimization procedure. It is worth to notice that considering the impact from different (less critical) direction would influence the results of the optimization procedure; however, the most significant and comprehensive configuration in terms of reduction of acceleration peaks and increase of energy absorption characteristics is the one obtained considering the most critical impact condition, which is the one investigated in this work.

3. New polymeric shock absorbers: numerical procedure description

The identification, the verification and the optimization of the behaviour of the proposed additive manufactured polymeric shock absorbers is carried out through numerical CAD and FEM activities.

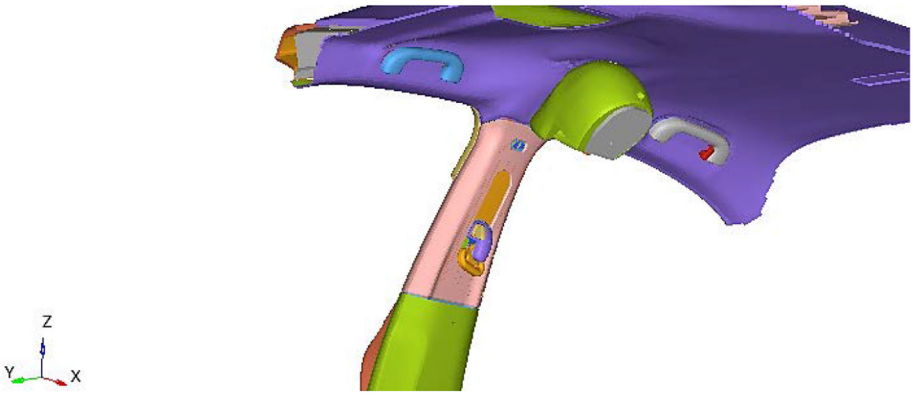

Figure 4. Upper Roof impact simulation without shock absorbers.

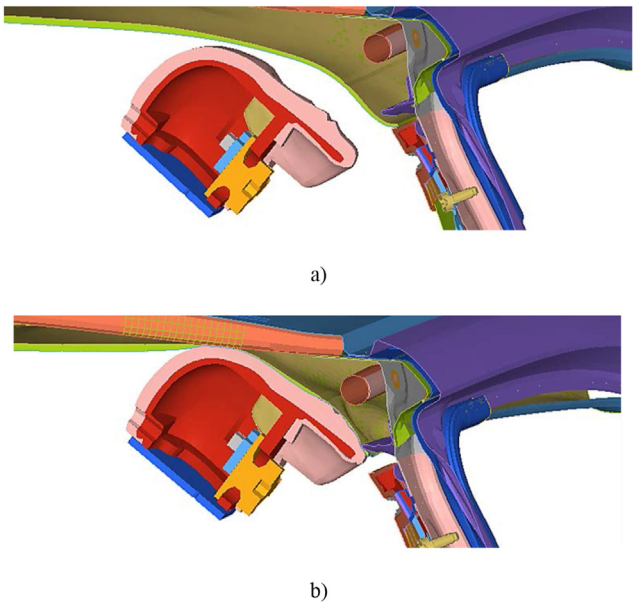

a)

b)

Figure 5. First Virtual Simulation without shock absorbers: a) Initial Configuration; b) Post impact configuration.

Actually, in the FEM pre-processing phase, the geometry can be created or imported from other software that are dedicated to the Computer Aided Design. In the frame of this work, the geometry has been created with Altair Hypermesh. The FEM solver, used for the computations, is LS-DYNA [19, 20, 21], which is a Livermore Software Technology Corporation (LSTC) software; finally, as post-processor, HyperView has been used for the creation of contour plots and HyperGraph for 2D/3D plots, starting from the simulation data provided by LS-DYNA. Stresses, strains, and deformations have been plotted and examined to investigate the mechanical behaviour of the investigated structural components.

A first simulation without shock absorbers has been performed, in compliance with the regulations, in the chosen impact zone. The FEM analysis that has been performed considering the "Upper Roof" conditions with its vertical and horizontal impacting angle limits (Figure 4).

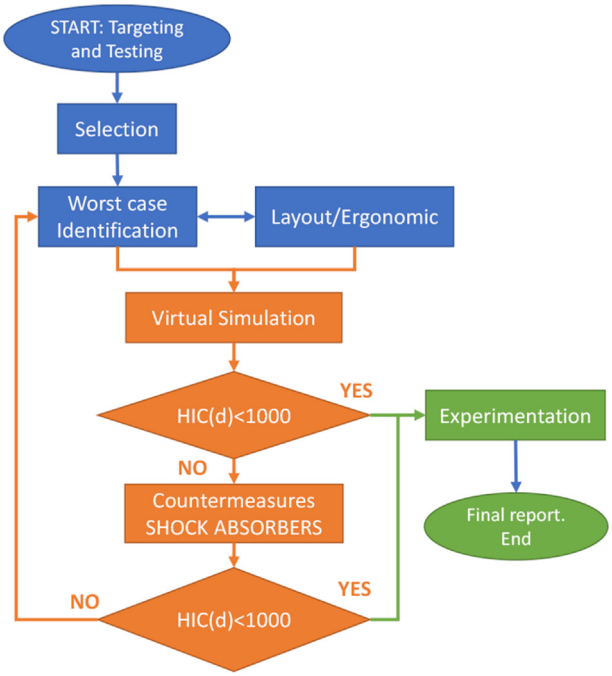

Figure 6. Automotive test phases.

Table 1. Roboze PP mechanical properties.

Mechanical Properties	Value	Unit
Tensile Strength	20	*MPa*
Modulus	1.62	*GPa*
Elongation (at break)	16%	
Density	0.9	g/cm^3

To reduce the computational cost, this first simulation has been performed only on the parts really affecting the impact phenomena under investigation. Indeed, preliminary analyses have been performed on the whole vehicle model in order to properly choose the reduced model by selecting only components reporting stress or deformations during the impact. Specifications on the end time, the output are requested such as: global data, material energy, data regarding nodal points and rigid bodies, and resultant interface forces. Also, information about the contact between the model of the car and the model of the Free Motion Headform (translation and rotation angles for example) and the initial FMH impact speed set to 6.7 m/s according to regulation, have been provided in input. In Figure 5, the results of the virtual simulation, in terms of deformed shapes, are shown for the initial and post-impact conditions.

After this preliminary simulation, the numerical activity in the frame of this research work has been performed consistently with the flow chart of Figure 6, showing the automotive test phases.

The diagram, in Figure 6, explains the logic behind the adoption of countermeasures such as shock absorbers. Shock Absorbers must be considered when the HIC index exceeds the regulations' limit.

The polymeric shock absorbers, considered in this research study, are supposed to be manufacture by the additive technique with a material system developed for the 3D Fused Deposition Modelling (FDM) printer Roboze ARGO 500 FDM. "Roboze PolyPropylene (PP)" is a polymer adopted for the production of consumer goods in several industrial sectors, thanks to its excellent chemical resistance, lightness, and impact resistance. In Table 1 the mechanical characteristics of the material are presented.

The proposed PP shock absorbers configuration has been finalized to protect the car occupants from impact against rigid zones. The numerical impact simulations with shock absorbers have been finalized, in the frame of an optimization analysis, to provide the best physical configuration and the best thicknesses combination to obtain the best HIC(d).

The optimization analysis has been performed by adopting the LS-OPT tool [22, 23] which is an optimization software interaction with LS-DYNA. Input for the LS-DYNA analyses are provided by the LS-OPT software, by means of an iterative procedure, to search for the best configurations. Optimal design means solving an optimization problem that incorporates design criteria as objectives or constraints. Some constraints have been applied by mathematical equations, based on experience, according to regulation requirements; while, the HIC(d) and the acceleration peak have been chosen as the objective functions to be minimized. A preliminary choice about the design parameters to be considered in the frame of the optimization study has been based on previous experiences on internal vehicle impacts.

As already mentioned, the technology used for the production of shock absorbers is the Additive Manufacturing, mainly because this technology [24] does significantly simplify the process of producing complex 3D objects directly from CAD data, by introducing approximations about the original geometry which have been considered acceptable for the application of interest. Indeed, In the FDM Additive Manufacturing process, components are generated by adding material as filaments; each filament has a thin cross-section and a weight, which will affect the theoretical geometry of the input CAD with a consequent approximation of the original geometrical data and a consequent use of supports during printing which need to be eliminated in a post-production phase. The thinner and the lighter each filament is, the

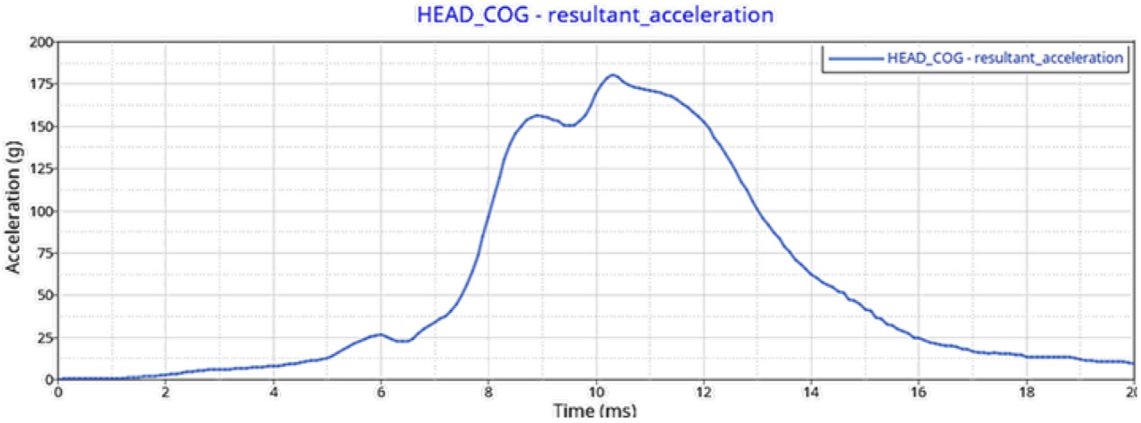

Figure 7. Acceleration-time graph for virtual simulation.

closer the final part will be to the original CAD design, but, at the same time, the longer will be the printing process.

AM involves a number of steps from the virtual CAD description to the physical part, which may include support cleaning, surface preparation, etc. The complexity of these steps are correlated to the material and to the geometry of the part to be produced.

4. New polymeric shock absorbers: numerical study, results and discussion

Once selected the upper roof impact as the most critical condition for the head internal vehicle impact, a numerical study has been performed to test the effectiveness of a new class of polymeric shock absorbers. In this section, the results from the three steps involved in the performed numerical study are presented: the virtual simulation of the upper roof impact without polymeric shock absorbers, the impact virtual simulation with polymeric shock absorbers, and the polymeric shock absorbers optimization analysis.

4.1. Virtual internal impact simulation without shock absorbers

As already mentioned in the previous section, a reduced FE model has been used, to decrease the computational effort. Instead of the whole vehicle, only the front upper part of the latter has been used for simulations. Indeed, as expected, it has been verified that most of the vehicle components do not experience any stress or deformation as a consequence of the head internal impact event. Hence, these parts have been deleted and substituted with constraints and rigid bodies; in particular, rigid bodies have been used to substitute the links between parts.

As a result of this first simulation, the deformed shape of Figure 5 has been found in HyperView, while, in Hypergraph, the FMH acceleration-time curve shown in Figure 7 has been extracted.

Table 2. Geometrical dimension shock absorbers.

Dimensions	Value
Anterior Absorber Width (w_a)	27 mm
Posterior Absorber Width (w_p)	31 mm
Anterior Absorber Height (h_a)	41 mm
Posterior Absorber Height (h_p)	48 mm
Anterior Absorber Bottom Radius (r_{a1})	23 mm
Posterior Absorber Bottom Radius (r_{p1})	24 mm
Anterior Absorber Top Radius (r_{a2})	15 mm
Posterior Absorber Top Radius (r_{p2})	15 mm
Absorbers Minimum Distance (d_{min})	14 mm
Absorbers Maximum Distance (d_{Max})	21 mm

The analysis, conducted with a 20 m s termination time, allowed to evaluate the HIC(d) value, which has been found equal to 1256.02. This value exceeds the regulation limit of 1000. Based on this first result, the adoption of countermeasures are needed to reduce the value of HIC(d); hence, polymeric shock absorbers have been introduced in the next virtual impact simulations.

4.2. Virtual internal impact simulation with polymeric shock absorbers

The second step of the accomplished numerical investigation was performed by introducing, as countermeasures, the proposed polymeric shock absorbers with a uniform thickness of 1.5 mm. The shock absorbers, made with Roboze PP have been meshed in Altair Hypermesh [25] environment. Mesh size is critical for impact testing analysis; it should be a good compromise between computational effort (which requires bigger elements) and good results (which requires smaller elements). For this purpose, the elements used are shell mixed elements sizing 4 mm for a total of 878 elements [26]. Table 2 shows the main geometrical dimensions of the shock absorbers configuration.

Figure 8 shows the shock absorbers arrangement hypothesized for the analysis.

Shock absorbers are connected to the vehicle imperial through a tied nodes to surface contact. Figure 9 shows the position where shock absorbers have been placed. In Figure 9b, results in terms of deformed shape for this second step of numerical simulations are plotted.

In Figure 10, the acceleration-time curve obtained in this second round of numerical simulations (the one with shock absorbers) is presented.

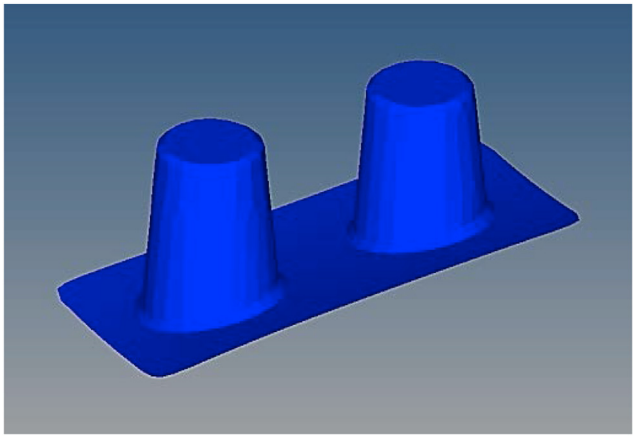

Figure 8. Shock absorbers model.

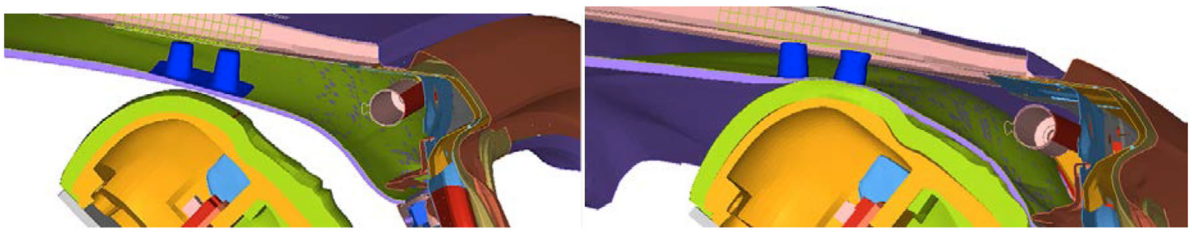

(a) (b)

Figure 9. Shock Absorbers: a) Initial configuration; b) Post-Impact configuration.

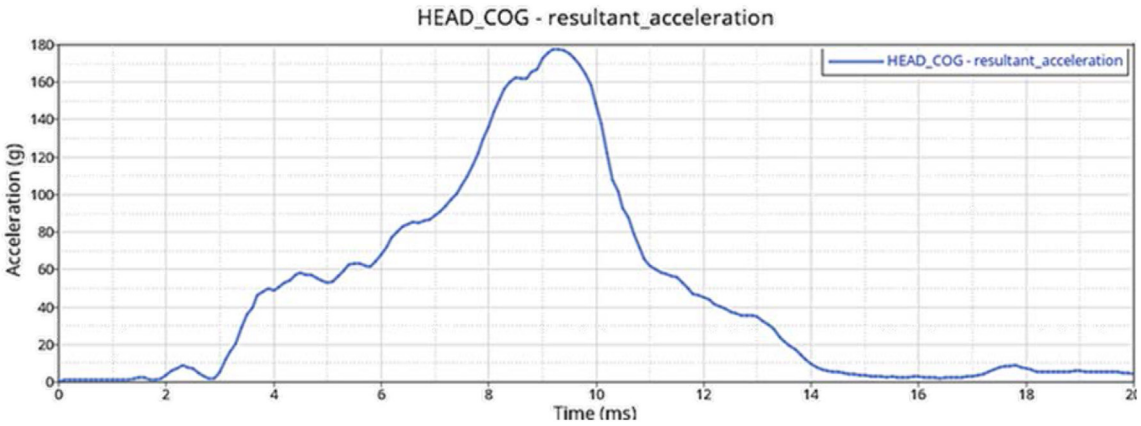

Figure 10. Acceleration-time graph for Configuration with shock absorbers.

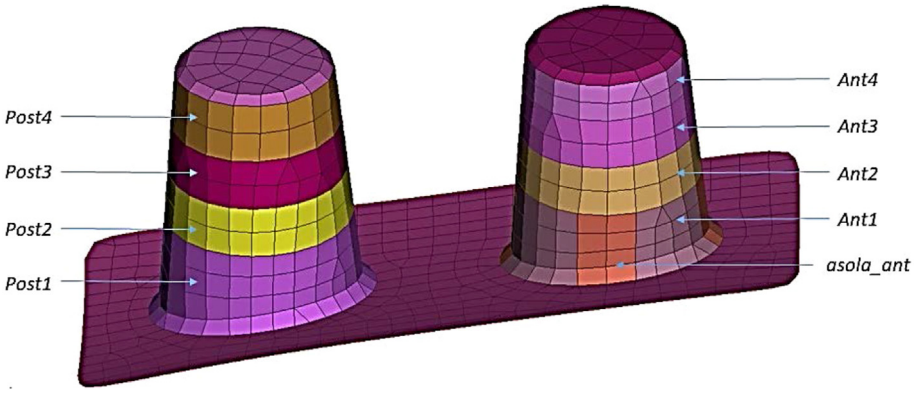

Figure 11. Shock absorbers sections.

A value of HIC(d) equal to 891 has been obtained in the frame of the simulations with PP shock absorbers with a uniform thickness of 1.5 mm. This value is below the regulations limit of 1000. This result is a first proof of the effectiveness of these shock absorbers. In order to improve the impact performance in terms of HIC(d), a third step involving an optimization by numerical FEM analyses has been performed. The optimization has been finalized to the determination of the best configuration, in terms of energy absorbing capability, of shock absorbers with variable thickness.

4.3. Optimization analysis and result

The optimization focused on the absorbers' geometry. The shock absorber introduced in the previous section demonstrates its capability to reduce the HIC parameter below the regulation limit; hence, the

Table 3. Ranges of thickness variation for the defined sections.

	Min	Max	Units
Post1	1	2	mm
Post2	1	2	mm
Post3	1	2	mm
Post4	1	2	mm
Ant1	1	2	mm
Ant2	1	2	mm
Ant3	1	2	mm
Ant4	1	2	mm
asola_ant	YES	NO	Boolean variable

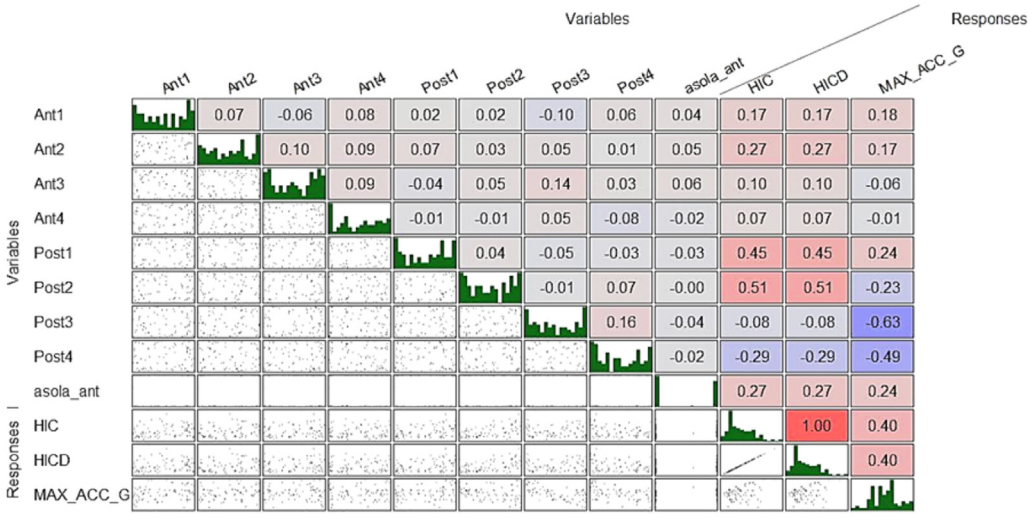

Figure 12. Correlation matrix.

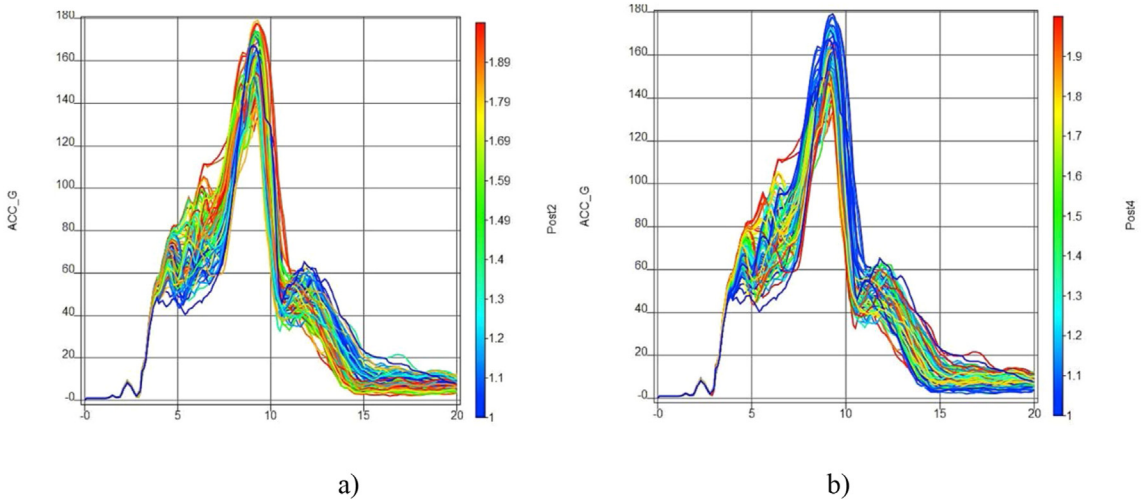

Figure 13. a) Max. Acceleration and Post2 Section Dependency; b) Max. Acceleration and Post4 Section Dependency.

configuration of the shock absorber, including its global dimension (i.e., height, length, radius of the absorbers) has been considered fixed. However, the performance in terms of reduction of HIC parameters and of acceleration peak could be further improved by adopting different thickness of the absorbers in key positions, which can be easily obtained without mouldings by additive manufacturing the component. Therefore, the two absorbers have been divided into sections, whose height has been defined according to manufacturability considerations. The thickness of each section has been optimized in the frame of the third round of impact simulations by means of the LS-OPT tool. The ranges of variation for the thickness of the different sections has been defined from 1 mm to 2 mm. Two possible discrete values, 0.2 mm and 1.5 mm, have been defined for

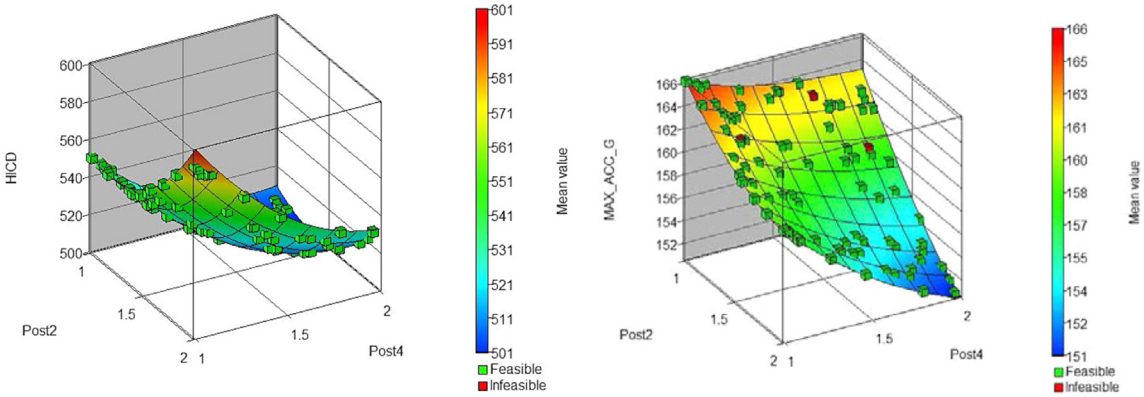

Figure 14. HIC(d) and maximum acceleration. meta-models.

Table 4. Optimum values.

	Optimal Design	Units
Post1	1	mm
Post2	1.36	mm
Post3	1.12	mm
Post4	2	mm
Ant1	1	mm
Ant2	1.28	mm
Ant3	1.87	mm
Ant4	1.81	mm
Asola_ant	0.2	mm

the "asola_ant" section, shown in Figure 11. Table 3 summarizes the ranges of variation for the sections defined.

A Radial Basis Function Network "RBF" with a Space filling point selection and 83 simulation points has been used in the sampling tab when defining the geometrical configurations to be used in the simulations. Key results, for this third round of analyses, are: the max acceleration in g units (multiplied by a factor of 1000/9.81), the HIC, and the HIC(d) values.

The results of the optimization are divided into four sections, but in this paper only two are used: Simulations and Metamodel. The simulations section describes the results of the experimental simulations, in this case 83 simulations as default. This section contains different graphs such as correlation matrix, scatter plots, histories, parallel coordinates.

In Figure 12, the correlation matrix is presented. This matrix shows, in the upper right area, how the responses are affected by the parameters. In particular, the red colour indicates a direct dependency while blue indicates an inverse dependency.

As shown in the correlation matrix, it can be noticed that the parameters, most affecting the HIC(d) and maximum acceleration, are the thicknesses of the shell "Post 2" and "Post 4". In particular, it can be noticed that there is a direct proportionality on Post 2 and an indirect proportionality on Post 4.

In Figure 13, the Histories, showing the graph for each acceleration depending on time for each simulation, are introduced (curve colours are associated to Post 2 and Post 4 variables). The trend highlighted in the correlation matrix is confirmed. Indeed, when Post 2 increases maximum acceleration increases, when Post 4 decreases maximum acceleration decreases. This is a demonstration of how these parameters dominate over others.

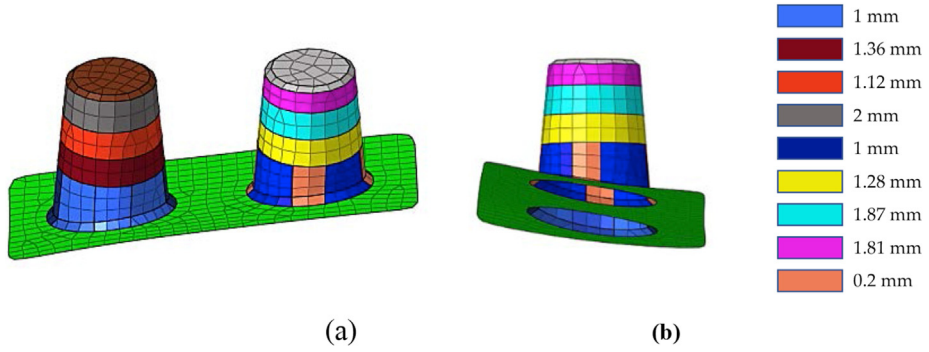

Figure 15. Shock absorber FEM: a) View in Y-Z plane; b) X-Z plane.

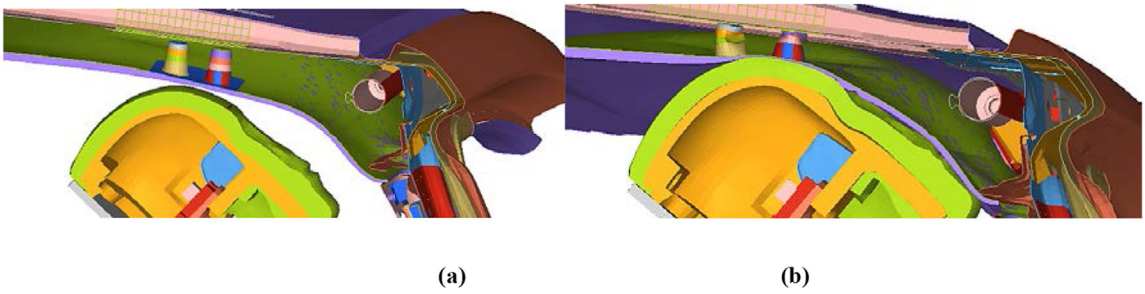

Figure 16. Shock absorbers: a) Time = 0 m s; b) Time = 7 m s

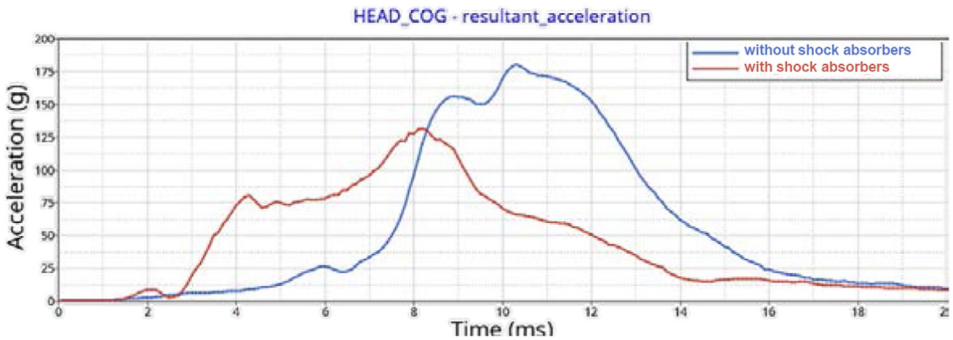

Figure 17. Comparison between configuration without shock absorbers and configuration with optimized shock absorbers.

Table 5. HIC(d) for the three main analysed configurations.

ANALYSIS	HIC(d)
Without Shock Absorbers	1256.02
With Shock Absorbers (uniform thickness t = 1.5 mm)	891
With Optimized Shock Absorbers	467.4

Concerning the Metamodel section, some interesting results have been predicted by interpolation of the results from the simulations. In Figure 14, the meta-model surfaces generated by the LS-OPT software can be appreciated. In Figure 14a and 14b, the HIC(d) and maximum acceleration, respectively, are shown as 3D graph as a function of the most influencing parameters Post 2 and Post 4.

From the meta-model section an optimal configuration has been chosen by performing a second iteration. Table 4 shows the optimal thickness values.

This optimal configuration of the designed polymeric shock absorbers has been implemented in FEM analysis. Figure 15 show the model with optimized thickness values.

Figure 16 shows the Hyperview output, in terms of deformed shapes, at the initial condition (time = 0) and at time = 7 m s.

The value of HIC(d) evaluated for optimized shock absorbers is 467.4, this value is an important result. Thanks to optimization analysis, the HIC(d) value has been halved. In Figure 17, the acceleration-time curve obtained with the optimized shock absorbers configuration is compared to the acceleration-time curve obtained without shock absorbers.

Table 5 shows the best result with optimized solution, in terms of HIC(d) value, compared to other solutions.

Optimized shock absorbers provide a percentage improvement, in terms of HIC(d) value, even over 63%. This result pushes towards the realization of the first prototype in Additive Manufacturing, that will be the starting step for the follow-on experimental research activity.

5. Conclusions

In this work, the "internal head impact" in the upper roof of automotive vehicle has been analysed. A study has been performed on the redesign of the upper roof by using shock absorbers, for the reduction of the HIC(d) "Head Injury Criteria". Three main configurations are analysed: a configuration without shock absorbers, a configuration with constant thickness shock absorbers and, finally, a configuration with optimized shock absorbers. Actually, an optimization analysis has been performed on the shock absorbers, showing that the HIC(d) values can be strongly reduced by differentiating and properly optimising the thickness of shock absorbers sections. A Polypropylene material systems for 3D FDM printers, has been selected for the proposed shock absorbers. Indeed, Additive Manufacturing has been considered the best manufacturing option to lower the costs, to create different shaped absorbers finalized to specific vehicle areas and to lower the vehicle weight. The work presented here, demonstrated the feasibility of such additive manufactured shock absorbers for automotive applications in future experimental phases.

Declarations

Author contribution statement

Aniello Riccio; Maria Domenica Madonna; Concetta Palumbo; Andrea Sellitto: Conceived and designed the experiments; Performed the experiments; Analyzed and interpreted the data; Contributed reagents, materials, analysis tools or data; Wrote the paper.

Funding statement

This research did not receive any specific grant from funding agencies in the public, commercial, or not-for-profit sectors.

Data availability statement

Data will be made available on request.

Declaration of interest's statement

The authors declare no conflict of interest.

Additional information

No additional information is available for this paper.

References

[1] T.F. MacLaughlin, R.A. Saul, S. Daniel, Causes and Measurement of Vehicle Aggressiveness in Frontal Collisions, Twenty-fourth Stapp Car Crash Conference, SAE Paper No. 801316, Troy, Michigan, 1980.
[2] T.F. MacLaughlin, R.A. Saul, R.M. Morgan, Vehicle Crashworthiness and Aggressiveness, VRTC Projects SRL-8 and SRL-9 Final Report, DOT HS 805 712 and DOT HS 805 713, 1981.
[3] Nanyu Jiang1, Runqi Qiu1, Modelling and simulation of vehicle ESP system based on CarSim and simulink, Journal of Physics: Conference Series, vol. 2170, in: 6th International Seminar on Computer Technology, Mechanical and Electrical Engineering (ISCME, 2021.
[4] Chirag Berry, Raj Rao, N. Yoganandan, Arnav agarwal, occupant and crash characteristics in thoracic and lumbar spine injuries resulting from motor vehicle collisions, Spine J. (2014).
[5] FCA ITALY S.p.A., Occupant Protection in Interior Impact, 2016.
[6] Vittorio Giavotto, Carlo Caprile, Alessandro Airoldi, et al., Research Activity at Politecnico di Milano Crash Test Laboratory, in: Third International Krash Users' seminar At: Arizona, USA, Crashworthiness and impact response of lightweight structures, 2001.
[7] Chris Coxon, Michael Paine, Jack Haley, Side Impacts And Improved Occupant Protection, Department of Transport & Urban Planning, South Australia, Vehicle Design & Research, NRMA Motoring and Services, Australia
[8] B. Henary, J. Crandall, K. Bhalla, C. Mock, B. Roudsari, Child and adult pedestrian impact: the influence of vehicle type on injury severity, in: 47th Annual Proceedings, Association for the Advancement of Automotive Medicine, 2003.
[9] Arun Chickmenahalli, Effectiveness of Countermeasures In Response to FMVSS 201 Upper Interior Head Impact Protection, Lear Corporation, Michigan, USA
[10] V. Jain, Z. Mujawar, Development of a free motion headform impactor, in: SAE Technical Paper 2011-26-0105, 2011.
[11] F. Mokhtarnezhad, S. Salehghaffari, M. Tajdari, Improving the crashworthiness characteristics of cylindrical tubes subjected to axial compression by cutting wide grooves from their outer surface, Int. J. Crashworthiness 14 (2009), 601611.
[12] M. Li, Z. Deng, R. Liu, H. Guo, Crashworthiness design optimisation of metal honeycomb energy absorber used in lunar lander, Int. J. Crashworthiness 16 (2011) 411–419.
[13] X. Yang, J. Ma, D. Wen, J. Yang, Crashworthy design and energy absorption mechanisms for helicopter structures: a systematic literature review, Prog. Aero. Sci. 114 (2020), 100618.
[14] V. Acanfora, R. Castaldo, A. Riccio, On the effects of Core microstructure on energy absorbing capabilities of sandwich panels intended for additive manufacturing, Materials 15 (4) (2022), 1291.
[15] K.V. Wong, A. Hernandez, A review of additive manufacturing, Int. Sch. Res. Notices 2012 (2012), 208760.
[16] N. Guo, M.C. Leu, Additive manufacturing: technology, applications and research needs, Front. Mech. Eng. 8 (2013) 215–243.
[17] U.S. Department Of Transportation, "Upper Interior Head Impact Protection"
[18] FCA ITALY S.p.A., Safety Compliance Testing for FMVSS 201, 2016.
[19] LSTC, LS-DYNA 3D Keyword User's Manual, 2007 version 971.
[20] J.O. Hallquist, LS-DYNA Theory Manual, LSTC, 2006.
[21] LSTC, LS-DYNA Database Binary Output Files, 2014.
[22] N. Stander, W. Roux, A. Basudhar, LS-OPT Training Class – Optimization and Robust Design, 2016.
[23] N. Stander, W. Roux, A. Basudhar, LS-OPT User's Manual, 2015.
[24] I. Gibson, D. W. Rosen & B. Stucker, "Additive Manufacturing Technologies"
[25] Altair Hyperworks guide, "Practical Aspects of Finite Element Simulation"
[26] R.D. Cook, Finite Element Modeling for Stress Analysis, J. Wiley & Sons Inc, 1995.